

Semaglutide lowers body weight in rodents via distributed neural pathways

Sanaz Gabery,¹ Casper G. Salinas,¹ Sarah J. Paulsen,¹ Jonas Ahnfelt-Rønne,¹ Tomas Alanentalo,¹ Arian F. Baquero,³ Stephen T. Buckley,² Erzsébet Farkas,³ Csaba Fekete,³ Klaus S. Frederiksen,¹ Wouter Frederik Johan Hogendorf,² Hans Christian C. Helms,² Jacob F. Jeppesen,¹ Linu M. John,¹ Charles Pyke,¹ Jane Nøhr,¹ Tess T. Lu,¹ Joseph Polex-Wolf,¹ Vincent Prevot,⁴ Kirsten Raun,¹ Lotte Simonsen,¹ Gao Sun,² Anett Szilvásy-Szabó,³ Hanni Willenbrock,² Anna Secher,¹ and Lotte Bjerre Knudsen¹

¹Global Drug Discovery and ²Global Research Technologies, Novo Nordisk A/S, Måløv, Denmark, and Seattle, Washington, USA. ³Institute of Experimental Medicine Hungarian Academy of Sciences, Budapest, Hungary. ⁴Inserm, Laboratory of Development and Plasticity of the Neuroendocrine Brain, Jean-Pierre Aubert Research Centre, Lille, France.

Semaglutide, a glucagon-like peptide 1 (GLP-1) analog, induces weight loss, lowers glucose levels, and reduces cardiovascular risk in patients with diabetes. Mechanistic preclinical studies suggest weight loss is mediated through GLP-1 receptors (GLP-1Rs) in the brain. The findings presented here show that semaglutide modulated food preference, reduced food intake, and caused weight loss without decreasing energy expenditure. Semaglutide directly accessed the brainstem, septal nucleus, and hypothalamus but did not cross the blood-brain barrier; it interacted with the brain through the circumventricular organs and several select sites adjacent to the ventricles. Semaglutide induced central c-Fos activation in 10 brain areas, including hindbrain areas directly targeted by semaglutide, and secondary areas without direct GLP-1R interaction, such as the lateral parabrachial nucleus. Automated analysis of semaglutide access, c-Fos activity, GLP-1R distribution, and brain connectivity revealed that activation may involve meal termination controlled by neurons in the lateral parabrachial nucleus. Transcriptomic analysis of microdissected brain areas from semaglutide-treated rats showed upregulation of prolactin-releasing hormone and tyrosine hydroxylase in the area postrema. We suggest semaglutide lowers body weight by direct interaction with diverse GLP-1R populations and by directly and indirectly affecting the activity of neural pathways involved in food intake, reward, and energy expenditure.

Introduction

Authorship note: SG, CGS, and SJP contributed equally to the work.

Conflict of interest: JAR, AFB, STB, KSF, JFJ, LMJ, CP, LS, AS, LBK, TTL, JP-W, HW, SG, CGS, GS, TA, HCCH, JN, and SJP are current or former Novo Nordisk employees and/or shareholders. CF and EF received research grants from Novo Nordisk to their institutions.

Copyright: © 2020, American Society for Clinical Investigation.

Submitted: September 17, 2019

Accepted: February 26, 2020

Published: March 26, 2020.

Reference information: *JCI Insight*. 2020;5(6):e133429. <https://doi.org/10.1172/jci.insight.133429>.

Six glucagon-like peptide 1 (GLP-1) receptor agonists (GLP-1RAs) are approved for the treatment of type 2 diabetes, including 4 long-acting agents, but only 1 (liraglutide) is approved and 1 (semaglutide) under investigation for the treatment of obesity. Both liraglutide and semaglutide are fatty acid acylated analogs of human GLP-1. In humans, the mechanism of action of liraglutide is primarily energy intake reduction (1). Semaglutide was primarily optimized to obtain a markedly longer half-life in humans (160 vs. 12 hours) and full dipeptidyl peptidase-4 stability (2). However, in randomized clinical trials in type 2 diabetes, semaglutide resulted in up to 3 times greater weight loss compared with other GLP-1RAs and up to twice as much in patients with obesity, approaching 15 kg (3–5). In small randomized controlled clinical trials, semaglutide lowered energy intake by, on average, approximately 25% over 3 meals (6) and liraglutide by approximately 15% over 1 meal (1). Semaglutide also lowered cardiovascular risk in patients with diabetes (7). Semaglutide is being investigated in 2 large phase III clinical trial programs in obesity: the STEP program, directed toward regulatory approval of semaglutide as an antiobesity drug, and SELECT (NCT03574597), evaluating cardiovascular outcomes in 17,500 patients. The mechanism of action of semaglutide in patients with obesity is similar to that of liraglutide — primarily energy intake reduction — but semaglutide has also been shown to improve control of eating and food cravings and reduce preference for fatty, energy-dense foods (6), suggesting that semaglutide may affect food intake via hedonic as well as homeostatic pathways.

We investigated the neural substrates mediating this effect. Peripherally administered liraglutide has direct access to a limited number of brain regions, primarily circumventricular organs and a few sites in the hypothalamus (8), and CNS GLP-1Rs are important for its body weight–lowering (BW-lowering) effect (9).

One challenge to elucidating a mechanistic role for GLP-1Rs stems from their complex expression across multiple brain regions (10–12), including the lateral septal nucleus (LSc), substantia nigra, ventral tegmental area (VTA), amygdala, nucleus accumbens (ACB), hippocampus, several regions of the hypothalamus (paraventricular nucleus of the hypothalamus [PVH], arcuate nucleus [ARH]), and hindbrain.

Following the original publication describing GLP-1 as a neurotransmitter involved in satiety (13), multiple efforts aimed to determine how neural GLP-1R populations interface with energy homeostasis pathways. GLP-1Rs in the hypothalamus and hindbrain have a role in satiety regulation and meal termination (8, 14–20); for example, this corresponds to a subset of anorexigenic cocaine- and amphetamine-regulated transcript (CART)/proopiomelanocortin (POMC) neurons that are directly targeted and activated by peripherally administered liraglutide (8). Other GLP-1R populations in the ACB, LSc, PVH, lateral hypothalamus (LHA), and VTA are involved in food choice, reward, and taste aversion (21–25). A growing body of evidence supports the hypothesis that GLP-1RAs may reduce food intake and BW through distributed effects in the CNS, rather than through a specific localized population of GLP-1Rs. Ablation of GLP-1Rs in the ARH does not fully attenuate the BW-lowering effect of liraglutide, suggesting that these GLP-1Rs are involved in, but not the sole mediators of, the effects of GLP-1RAs (20). Furthermore, the efficacy of liraglutide is not altered by area postrema (AP) or PVH ablation or by vagal lesions (8, 20). A study in genetically engineered mice highlighted that GLP-1Rs on glutamatergic (rather than GABAergic) neurons are required for liraglutide-induced weight loss (19). Several GLP-1R-positive neuronal populations in different locations could thus be involved, suggesting action on a network of neurons that likely interfaces with multiple aspects of neural energy homeostasis control.

We characterized how semaglutide interacts with different neural GLP-1R populations to affect BW, energy expenditure (EE), and food preference. Our data show that semaglutide did not permeate the blood-brain barrier (BBB); it affected the brain via circumventricular organs and may work through select regions close to the ventricles, such as the LSc and ARH. In the ARH, semaglutide — similarly to liraglutide — directly activates POMC/CART neurons. Semaglutide distribution is limited to discrete brain regions, with some differences compared with liraglutide, i.e., in the PVH and LSc. Using complementary approaches, we identified direct and indirect effects of semaglutide on neuronal activity and gene expression. Characterization of the phenotypes of GLP-1R neurons in areas directly targeted by semaglutide revealed that proteins known to be involved in appetite regulation coexpress with GLP-1R. The transcriptomic effects of liraglutide and semaglutide were evaluated in 6 rat brain nuclei involved in energy homeostasis control. Differential regulation of gene pathways between liraglutide and semaglutide matched differences in compound distribution. Semaglutide increased prolactin-releasing peptide (PrRP) and tyrosine hydroxylase (TH) in the hindbrain. These data, combined with an automated analysis of whole-brain c-Fos activity showing sites with and without direct compound access, support a model in which semaglutide regulates BW by directly targeting independent brain regions; through these entry sites, multiple pathways are engaged in providing input to key appetite-modulating relay stations, such as the parabrachial nucleus (PB). We provide a potentially novel, comprehensive view of the direct and indirect effects of peripherally administered, long-acting GLP-1RAs on multiple brain regions. Building upon previous attempts to characterize essential cell populations, we elaborate on neuronal populations and pathways that engage with GLP-1RAs and, thus, may explain overall pharmacologic efficacy. Compared with genetic approaches highlighting the importance of single GLP-1R populations, this broader approach is important in determining the functional mechanisms of GLP-1RAs and evaluating the potential translational value of other mechanistic principles for the treatment of obesity.

Results

Semaglutide induces weight loss, lowers food intake, and alters food preference in diet-induced obese rodents. Diet-induced obese (DIO) mice and rats fed a high-fat diet received semaglutide, administered subchronically, and the effects on food intake and BW were evaluated. In a 3-week study in DIO mice, semaglutide dose-dependently reduced BW and suppressed food intake. The reduction in BW from baseline was 22% at the maximum dose tested (mean \pm SEM, 100 nmol/kg from 43.6 ± 1.6 g to 34.8 ± 1.4 g) and 10% from baseline at the lowest dose tested (mean \pm SEM, 1 nmol/kg, from 42.5 ± 1.3 g to 38.2 ± 1.3 g) (Figure 1, A and B). In addition to the changes in BW, reductions in fat mass were observed (Supplemental Figure 1; supplemental material available online with this article; <https://doi.org/10.1172/jci.insight.133429DS1>). In contrast, the effect on lean mass was minor and not significant relative to vehicle control (Supplemental Figure 1). Maximal suppression of food intake occurred within the first 5 days, with the greatest reduction in food intake observed on day 1 at the highest dose of semaglutide (mean \pm SEM, 100 nmol/kg dose,

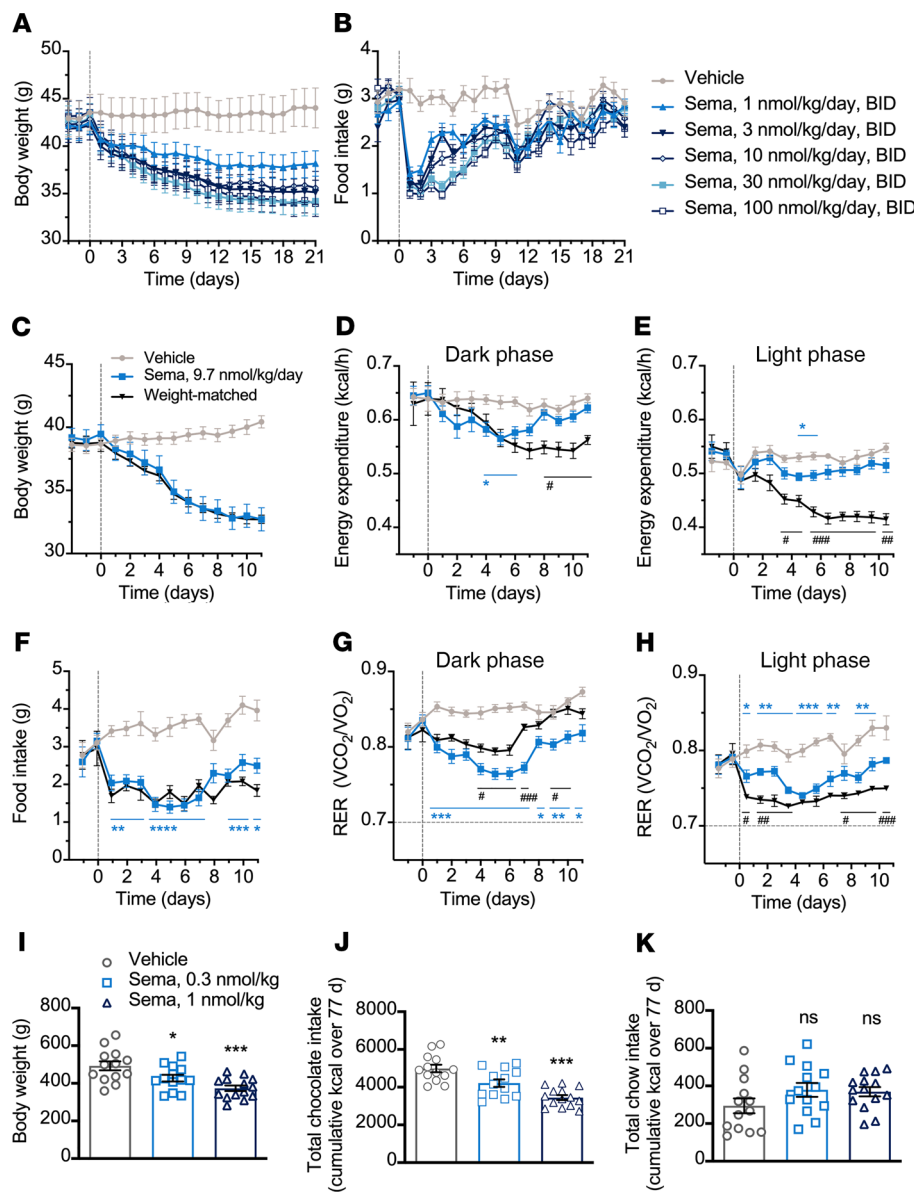


Figure 1. Semaglutide in obese rodents. (A and B) BW and food intake in DIO mice treated twice daily ($n = 9$). (C–H) BW, EE, food intake, and RER in DIO mice treated once daily ($n = 8$). * $P < 0.05$, ** $P < 0.01$, *** $P < 0.001$, and **** $P < 0.0001$ semaglutide (sema) vs. vehicle and $^{\#}P < 0.05$, $^{\#\#}P < 0.01$, and $^{\#\#\#}P < 0.001$ sema vs. weight-matched, mixed-effects model, Tukey's post hoc. (I–K) BW and food preference in DIO rats treated once daily ($n = 13$ –14). * $P < 0.05$, ** $P < 0.01$, and *** $P < 0.001$ vs. vehicle, 1-way ANOVA, Dunnett's post hoc. Data are individual measures with mean \pm SEM. Animals were subject to a 12-hour light/12-hour dark cycle. RER, respiratory exchange ratio; sema, semaglutide.

reduction of $68.2\% \pm 4.3\%$ compared with vehicle). A similar pattern of BW loss and transient food intake suppression was observed in DIO rats (data not shown).

To evaluate the effect of semaglutide on energy balance and substrate use, DIO mice that received vehicle or semaglutide (9.7 nmol/kg) for 11 days were assessed using indirect calorimetry. Food-restricted, weight-matched controls were used as comparators. Semaglutide suppressed food intake and induced a 17%–18% reduction in BW (Figure 1, C and F). No significant changes in locomotor activity were observed between groups (Supplemental Figure 1). Weight-matched controls responded to food restriction with a sustained reduction in EE during the dark and light phases (animals were subject to a 12-hour light/12-hour dark cycle) (Figure 1, D and E). In contrast, semaglutide transiently reduced dark phase EE until day 6 of treatment, after which levels were not significantly lower than those of the vehicle-treated controls (Figure 1D). Using ANCOVA to adjust EE for lean mass after treatment, we found no difference between semaglutide and vehicle control (Supplemental Figure 1). Reduction in the RER occurred following semaglutide and food restriction (Figure 1, G and H). During the dark phase, the reduction in RER with semaglutide was more pronounced than with weight-matched controls; the converse was true during the light phase. This corresponded to the observation that all weight-matched controls consumed all food within the first few hours of the dark phase, whereas in the semaglutide group, food intake was more gradual, occurring throughout the dark phase.

The effect of semaglutide on preference for palatable food was tested in a 77-day study in rats simultaneously offered standard chow and chocolate bars. There was a significant and dose-dependent reduction in BW (Figure 1I, $P < 0.05$ for 0.3 nmol/kg semaglutide; $P < 0.001$ for 1 nmol/kg semaglutide) in semaglutide-treated animals compared with controls. The reduction in energy intake was driven by decreased chocolate intake with semaglutide treatment compared with vehicle (Figure 1J, $P < 0.01$ for 0.3 nmol/kg semaglutide, $P < 0.001$ for 1 nmol/kg semaglutide). Meanwhile, there was a nonsignificant increase in chow intake with semaglutide compared with control (Figure 1K).

Semaglutide specifically accesses GLP-1R-positive brain areas following peripheral administration. Mice received VivoTag750-S-labeled semaglutide (semaglutide^{VT750}) and were compared with vehicle-injected mice (Figure 2C). Whole-brain data acquisition was performed with light sheet fluorescence microscopy to detect fluorescent signals with acute (6 hours i.v.) and steady-state (5 days, once daily s.c.) semaglutide^{VT750} and quantified using a digital brain atlas. Following acute administration, a robust signal for semaglutide^{VT750} was observed in 4 circumventricular organs: AP, median eminence (ME), vascular organ of the lamina terminalis (OV), and subfornical organ (SFO); as well as in regions protected by the BBB: the caudal part of the LSc, septofimbrial nucleus (SF), ARH including the posterior part (PVp), median preoptic nucleus, nucleus tractus solitarius (NTS), and the dorsal motor nucleus of the vagus nerve (DMX). Semaglutide^{VT750} was also observed in the choroid plexus (CHPL), as exemplified by the plexus located in the lateral ventricle (Figure 2, A and D). At steady state, semaglutide^{VT750} was also apparent in the dorsomedial hypothalamic nucleus (DMH), medial mammillary nucleus (MM), PVH, supraoptic nucleus (SO), and tuberal nucleus (TU) (Figure 2, B and E).

To evaluate whether the semaglutide^{VT750} signal was dependent on GLP-1R expression, semaglutide^{VT750} was administered to mice lacking a functional GLP-1R (*Glp1r*^{-/-}) and evaluated after 6 hours. Visually, the average distribution signals clearly decreased in all brain regions except the CHPL in the *Glp1r*^{-/-} group (Figure 2F). GLP-1R was visualized using whole-brain GLP-1R IHC staining (Figure 2G) and compared with the steady-state semaglutide^{VT750} signal. There was a high degree of overlap between semaglutide and receptor distribution, mainly in hypothalamic and hindbrain regions. Supplemental Video 1 shows semaglutide^{VT750} distribution in the mouse brain at steady state.

Differences in the central distribution of semaglutide^{VT750} and liraglutide^{VT750} were compared at steady state in mice. Signal intensities in multiple regions obtained from the whole-brain access data (semaglutide^{VT750}; Figure 2, B and F; liraglutide^{VT750}; Supplemental Figure 2) showed areas with increased semaglutide^{VT750} access compared with liraglutide^{VT750}, namely the LSc, SF, MM, and PVp, and areas showing the converse (OV, SO, PVH, and SFO; Figure 2H). High-resolution confocal image analysis following administration of cyanine 3-labeled semaglutide and liraglutide (semaglutide^{Cy3} and liraglutide^{Cy3}) to mice qualitatively showed the differences in distribution pattern in the hypothalamus and AP (Figure 3, A–J). Both compounds were present in the ARH, but compared with liraglutide^{Cy3}, semaglutide^{Cy3} had a distribution that extended more laterally (Figure 3, A–C and F–H) and further into the posterior portions (Figure 3, C and H) of the ARH. In the AP, both compounds were equally distributed (Figure 3, D and I), whereas in the PVH, liraglutide^{Cy3} extended more laterally, compared with semaglutide^{Cy3} (Figure 3, E and J).

Semaglutide does not interact with endothelial cells of the BBB. Using electron microscopy, GLP-1R expression in rat tissue was detected within α tanycytes, neuronal perikarya, and dendrites, with more limited staining in β_2 tanycytes. Notably, there was no labeling on endothelial cells of capillaries in the ARH (Figure 4, E and F). Endothelial/astrocyte cocultures and rat neonatal tanycyte primary cultures were used as *in vitro* models with previously documented properties reflecting the BBB biology (26–28). Semaglutide^{Cy3} (100 nM) showed no specific accumulation in endothelial cells whereas, in tanycytes, heterogeneous accumulation was observed (Figure 4G). Coincubation with the GLP-1 antagonist exendin 9-39 (1000 nM) abolished most of the signal in tanycytes. GLP-1R expression and activation were investigated in tanycytes by determining phosphorylation of the cyclic AMP response element binding protein (p-CREB) (Supplemental Figure 3). In controls, a few nuclei stained weakly positive, indicating constitutive p-CREB. Incubation with 100 nM semaglutide induced p-CREB expression in all nuclei, a response inhibited by coincubation with 1000 nM exendin 9-39, indicating that semaglutide binds to and activates GLP-1Rs on tanycytes. IHC with an antibody recognizing mouse and rat GLP-1R showed expression in cultured tanycytes, whereas no signal was seen in endothelial cells isolated from rat cortices or in secondary antibody controls (Supplemental Figure 4).

Radiolabeled semaglutide (¹²⁵I-semaglutide) in the presence and absence of exendin 9-39 was used

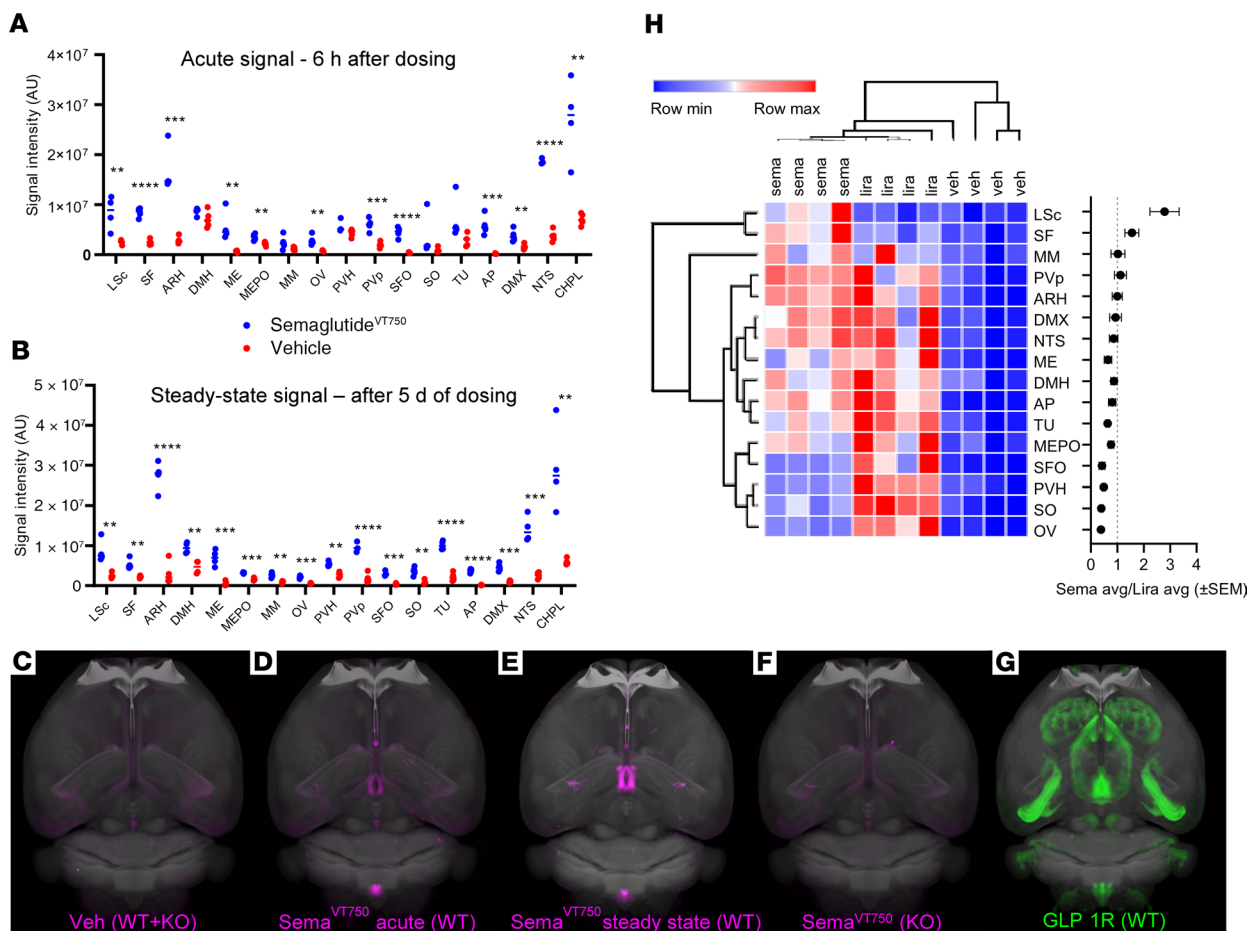


Figure 2. Semaglutide^{VT750} distribution in mouse brain. (A) Acute and (B) steady-state brain distribution. Dots show individual measures of total fluorescence signal in selected brain regions with horizontal bar at group median. Asterisks indicate enriched regions with FDR of 5%; ** $P \leq 0.01$; *** $P \leq 0.001$; **** $P \leq 0.0001$. (C–F) Maximum intensity projection (MIP) of the average signal computed from individual brains ($n = 4$) overlaid onto the Common Coordinate Framework version 3 template from AIBS. (C) Representative vehicle signal from WT and *Glp1r^{-/-}* mice. (D) Acute semaglutide^{VT750} signal, WT mice. (E) Steady-state semaglutide^{VT750} signal, WT mice. (F) Acute semaglutide^{VT750} signal, KO mice. (G) GLP-1R distribution visualized with whole-brain IHC. (H) Clustered heatmap of fluorescence signal in selected brain regions from mice treated with semaglutide^{VT750}, liraglutide^{VT750}, or vehicle ($n = 4$). Plot shows average semaglutide^{VT750} versus liraglutide^{VT750} signal per region. Regions selected based on at least 2.5-fold signal enrichment over vehicle-treated animals in either semaglutide- or liraglutide-treated groups. Hierarchical clustering of samples (columns) and brain regions (rows) based on Pearson's correlation. AIBS, Allen Institute for Brain Science; DMH, dorsomedial hypothalamic nucleus; FDR, false discovery rate; lira, liraglutide; liraglutide^{VT750}, VivoTag750-S-labeled liraglutide; max., maximum; MEPO, median preoptic nucleus; min., minimum; MM, medial mammillary nucleus; PVH, paraventricular nucleus of the hypothalamus; PVP, posterior part; semaglutide^{VT750}, VivoTag750-S-labeled semaglutide; SO, supraoptic nucleus; TU, tuberal nucleus; Veh, vehicle.

to quantify the semaglutide that interacts with the BBB endothelium and tanyocytes (Figure 4, H and I). Uptake of semaglutide was significantly higher in tanyocytes than endothelial cells ($P < 0.0001$). Exendin 9-39 partly inhibited tanyctic uptake of ^{125}I -semaglutide ($P < 0.01$) but did not affect uptake in endothelial cells (Figure 4H). The ability of tanyocytes to release semaglutide was studied by preloading them with ^{125}I -semaglutide and applying clean uptake buffer to obtain an outgoing concentration gradient (Figure 4I). Intracellular accumulation of ^{125}I -semaglutide declined after removal of the donor medium, resulting in a 66% reduction in the accumulated compound after 15 minutes.

GLP-1R-expressing neurons in the ARH and AP coexpress genes involved in appetite regulation and take up semaglutide. The cellular phenotypes of GLP-1R-expressing cells in the ARH and AP were evaluated by costaining for GLP-1R and markers of appetite regulation. GLP-1R was coexpressed with CART in the ARH (Figure 5A) but not in the AP or NTS (Supplemental Figure 5). GLP-1R was highly coexpressed with somatostatin (SST), a marker of GABAergic neurons, in the ARH (Figure 5B) and the LSc, but not in the AP or NTS (Supplemental Figure 6). In recent studies, TH-expressing neurons in the ARH, coexpressing neither neuropeptide Y (NPY)/agouti-related peptide (AgRP) nor CART, were implicated in metabol-

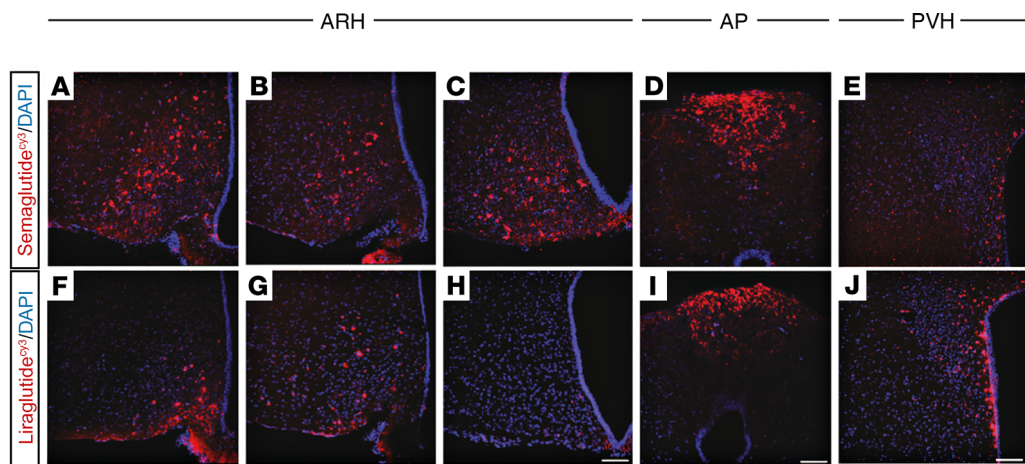


Figure 3. Differential distribution of semaglutide^{Cy3} and liraglutide^{Cy3} in the hypothalamus and AP. Representative high-magnification confocal images from mice injected for 4 consecutive days with semaglutide^{Cy3} or liraglutide^{Cy3} (red, each $n = 3$); DAPI nuclear stain (blue). (A–C and F–H) ARH, 3 different levels from an anterior to posterior direction; (D and I) AP; and (E and J) PVH. Scale bar: 100 μ m.

ic control (29). A sparse overlap between GLP-1R and TH was observed in the ARH, while in the AP coexpression was abundant (Figure 5, C and D). The uptake of semaglutide^{Cy3} into the abovementioned neuronal populations was examined. In the ARH, semaglutide colocalized with GLP-1R (Figure 5, E–H), CART (Figure 5I), SST (Figure 5J), and TH (Figure 5K). Similarly, semaglutide^{Cy3} and TH colocalized in the AP (Figure 5L). These data demonstrate that peripherally injected semaglutide enters GLP-1R-positive neurons, which likely interface with central appetite regulation pathways.

Semaglutide stimulates neuronal activity in brain areas involved in appetite regulation. Current clamp recordings from mouse brain ARH slices containing POMC–enhanced green fluorescent protein and NPY–humanized Renilla green fluorescent protein neurons were performed, and changes in membrane potential were measured in the absence and presence of semaglutide. POMC/CART neurons were depolarized in response to semaglutide, whereas NPY/AgRP neurons elicited membrane hyperpolarization and became inactivated (Supplemental Figure 7, A–F). Semaglutide further altered expression of POMC and NPY neuropeptides, as measured by quantitative PCR following laser capture microdissection of the ARH from DIO mice subchronically administered semaglutide. Both NPY and AgRP mRNA levels were higher in weight-matched controls than in the semaglutide-treated group (NPY 1.3-fold, $P < 0.01$; AgRP 1.5-fold, $P < 0.05$) and the ad libitum vehicle-fed controls (NPY 2-fold, $P < 0.001$; AgRP 2.8-fold, $P < 0.001$; Supplemental Figure 7G). CART mRNA levels were increased in semaglutide-treated mice compared with the vehicle-fed mice (1.2-fold, $P < 0.05$) and weight-matched mice (1.7-fold, $P < 0.001$), whereas POMC expression was unaffected (Supplemental Figure 7G).

c-Fos expression in the brain was quantified using automated segmentation methodology 4 hours after subcutaneous (s.c.) injection of semaglutide or vehicle. Increased c-Fos activity was observed in the bed nuclei of the stria terminalis (BST), central amygdala nucleus (CeA), OV, parasubthalamic nucleus (PSTN), SFO, midline group of the dorsal thalamus (MTN), PB, AP, DMX, and NTS after acute s.c. semaglutide (4 hours) (Figure 6, A–C). When an average heatmap of semaglutide-specific c-Fos increase (Figure 6B) was compared visually with the map of semaglutide^{WT/WT} brain access (Figure 2E), the largest overlap was in the hindbrain, mainly in the AP and NTS, indicating that the c-Fos response was a direct effect of semaglutide interaction with GLP-1R in these regions (Figure 6D). However, most of the c-Fos increase occurred in regions not directly targeted by semaglutide (BST, CeA, MTN, PB, and PSTN), indicating secondary activation. These areas corresponded to regions identified as being part of an appetite regulation pathway related to meal termination (30–33). This pathway is believed to be initiated by hindbrain signaling and relayed through the lateral PB. Further investigation of the semaglutide-induced c-Fos signal in the lateral PB revealed distinct c-Fos expression in 2 subnuclei: the central lateral (cl) and dorsal lateral (dl) PB. Costaining for c-Fos and the appetite-suppressive protein, calcitonin gene-related peptide (CGRP), revealed a high degree of overlap in dl PB and none in cl PB (Supplemental Figure 8). Furthermore, a c-Fos–negative, CGRP-positive cell population was observed in the external lateral PB (Supplemental Figure 8).

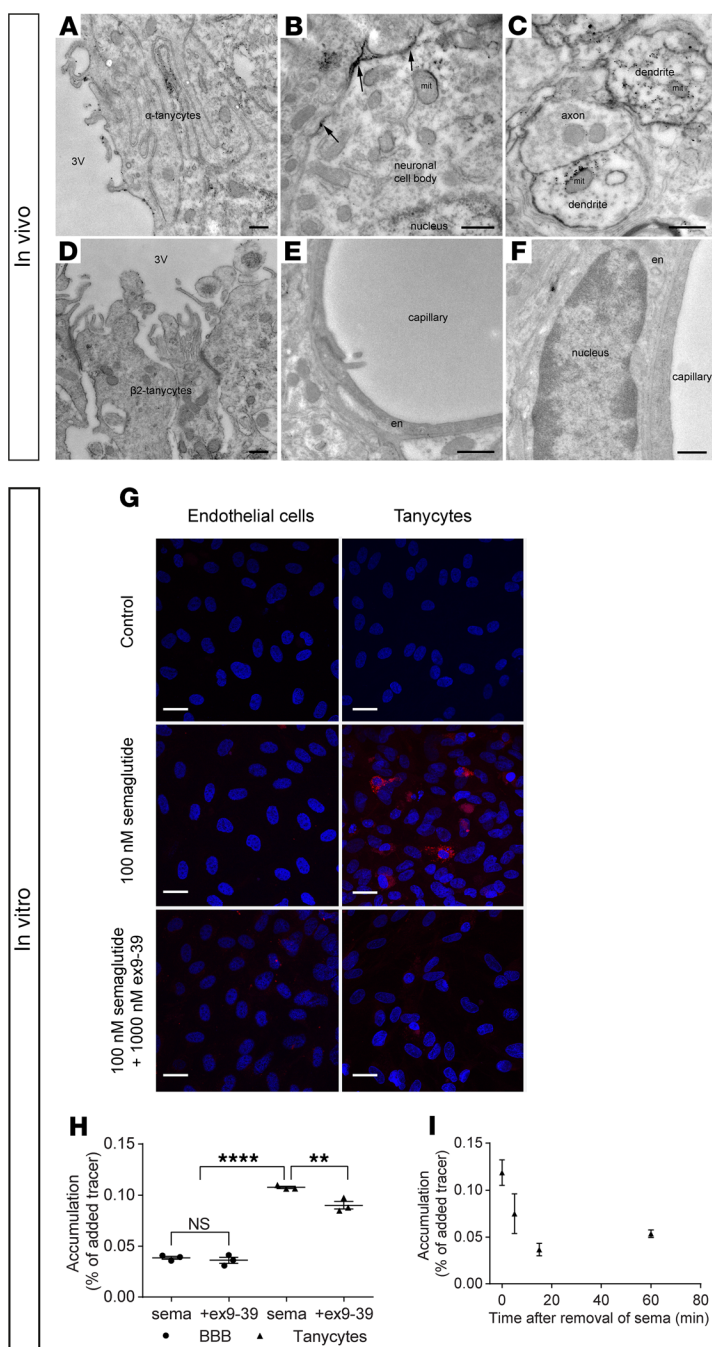


Figure 4. GLP-1R is present on tanyocytes but not endothelial cells in rat ARH, and in vitro, semaglutide does not interact with BBB endothelial cells but is taken up by tanyocytes. Electron micrographs of rat tissue section from the ARH showing GLP-1R immunoreactivity (silver grains) on (A) the ventricular surface and interwoven lateral surface of α tanyocytes, (B) the cell membrane of neuronal perikarya (arrows), and (C) the cytoplasm and surface of dendrites. (D) Limited, scattered GLP-1R immunoreactivity in β_2 tanyocytes lining the ventricular wall of the ME. (E and F) Endothelial cells lining capillaries in the ARH appear unlabeled. (G) Semaglutide^{Cys} (100 nM; in red) uptake in bovine brain endothelial cells (left column) in coculture with rat astrocytes and in rat tanyocytes in monoculture (right column), with or without 1000 nM exendin 9-39 (ex-9-39). Nuclei Hoechst staining (blue). (H) Intracellular accumulation of ^{125}I -semaglutide (0.7 nM) in BBB endothelial cells and tanyocytes with or without 1000 nM ex-9-39. Individual values, mean, and SD shown ($n = 3$). Means were compared using 2-way ANOVA with Bonferroni's correction. ** $P < 0.01$, and **** $P < 0.0001$. (I) Intracellular accumulation of ^{125}I -semaglutide in preloaded tanyocytes in clean uptake buffer. Data are shown as mean and SD ($n = 3$). Scale bars: 500 nm (A–F), 25 μm (G). en, endothelial cell; 3V, third ventricle; mit, mitochondrion.

A contextual relationship between whole-brain c-Fos activation and semaglutide was established by comparing the semaglutide-specific c-Fos heatmap (Figure 6B) with 2469 brain connectivity maps from the AIBS. The largest overlap originated from the NTS or PB (Supplemental Table 1). A connectivity map of glutamatergic projections from the PB was overlaid with the semaglutide-specific c-Fos–generated heatmap to visualize the likely involvement of the observed regions with secondary brain activation (Figure 6E).

To further characterize GLP-1RA stimulation of glutamatergic projections from the hindbrain to the PB, we examined the expression of the vesicular glutamate transporter SLC17A6 (also known as vGLUT2), which mediates glutamate uptake in excitatory neural cells, and GLP-1Rs in the AP and NTS. In the AP, overlap between SLC17A6 and GLP-1R was observed, whereas there were no GLP-1R–positive cell bodies in the NTS, suggesting that the glutamatergic entry point for GLP-1RAs to the PB is through the AP (Supplemental Figure 9). Supplemental Video 2 shows acute neuronal activation, based on c-Fos staining following semaglutide administration.

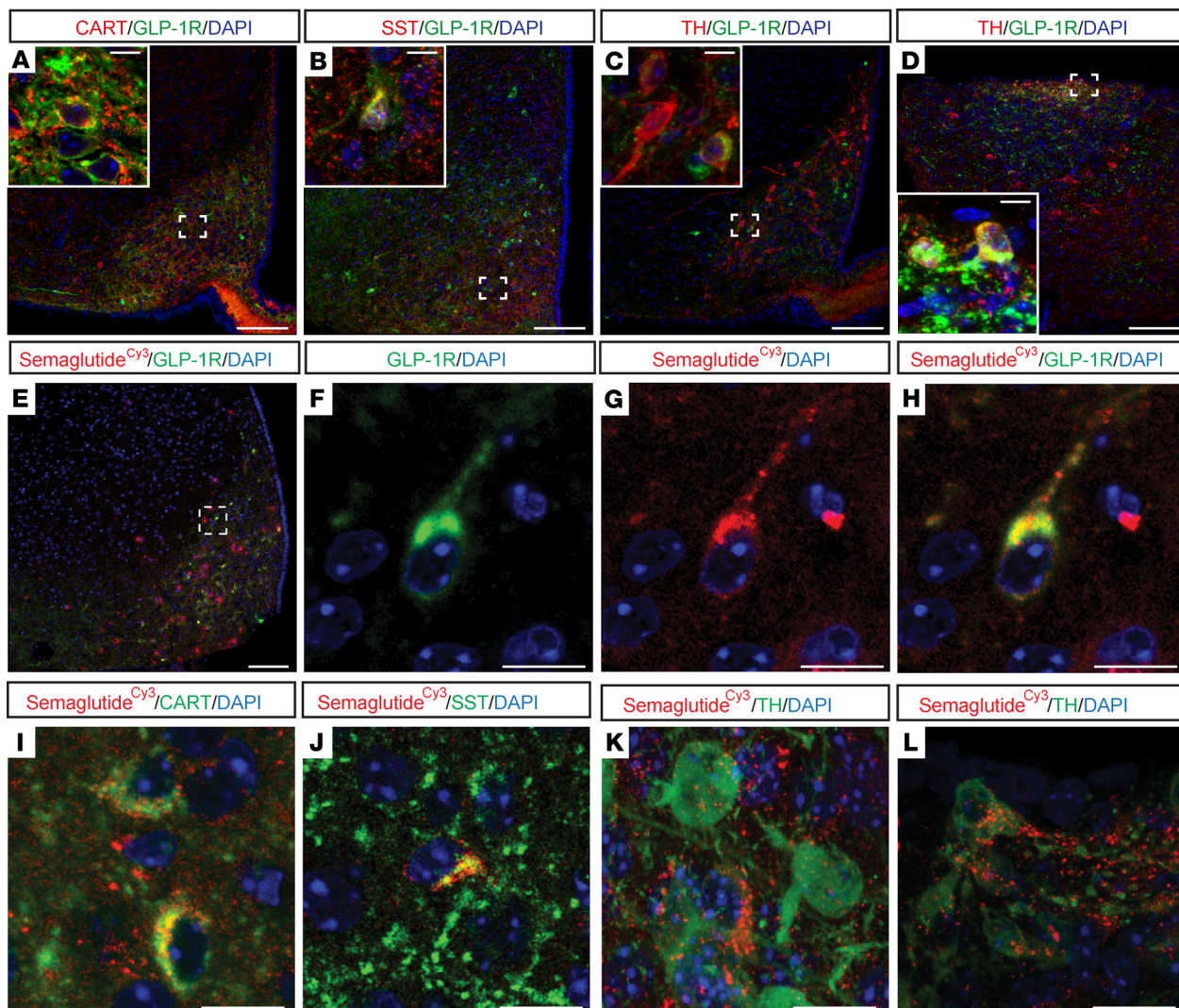


Figure 5. GLP-1R neurons coexpress modulators of appetite regulation in areas directly targeted by peripheral administration of GLP-1RAs. (A–H) Representative immunofluorescence images taken from mouse ARH and AP processed for GLP-1R (green) and CART, SST, and TH, respectively (red). DAPI nuclear staining (blue). GLP-1R expression in (A–C) ARH, colocalized with CART, SST, and TH, respectively, and in (D) AP colocalized with TH. Dashed boxes indicate the location of the insets. (E–L) Confocal images from mice i.v. injected for 4 consecutive days with semaglutide^{Cy3} (red) and DAPI nuclear stain (blue) applied. (E–H) Colocalization of semaglutide^{Cy3} with GLP-1R in the ARH. Dashed box in E indicates location of F–H. (I–K) Colocalization of semaglutide^{Cy3} with CART, SST, and TH, respectively, in the ARH and (L) with TH in AP. Scale bars: 100 μ m (A–E), 10 μ m (A–D insets and F–H), and 20 μ m (L). SST, somatostatin.

Transcriptomic effects of semaglutide and liraglutide in discrete brain regions. Effects on mRNA profiles were examined in 6 laser capture microdissected brain regions (LSc, PVH, ARH, DMH, AP, and NTS), based primarily on areas with compound and receptor distribution overlap. RNA sequencing gene expression analyses were performed in semaglutide- and liraglutide-treated DIO rats after weight loss, during the steady-state weight maintenance period. A comparable level of weight loss between treatment groups was achieved via dose adjustment. Treatment groups were compared with an ad libitum vehicle-fed group and a weight-matched control group, to differentiate between the effects of weight loss induced by food restriction and GLP-1RA treatment (Supplemental Figure 10A).

Genes with well-established spatial expression patterns were used to assess sample purity and indicated successful microdissection (Supplemental Figure 10B), mirrored by clear segregation of the 6 different brain regions in a principal component analysis (Supplemental Figure 10C). Within the 6 brain regions, no clear differences between treatment groups was observed (Supplemental Figure 10B). A limited number of statistically significant differentially expressed genes (DEGs) were identified by analysis of gene expression between treatment groups for each area (Supplemental Table 2). Supplemental Table 3 shows raw data for

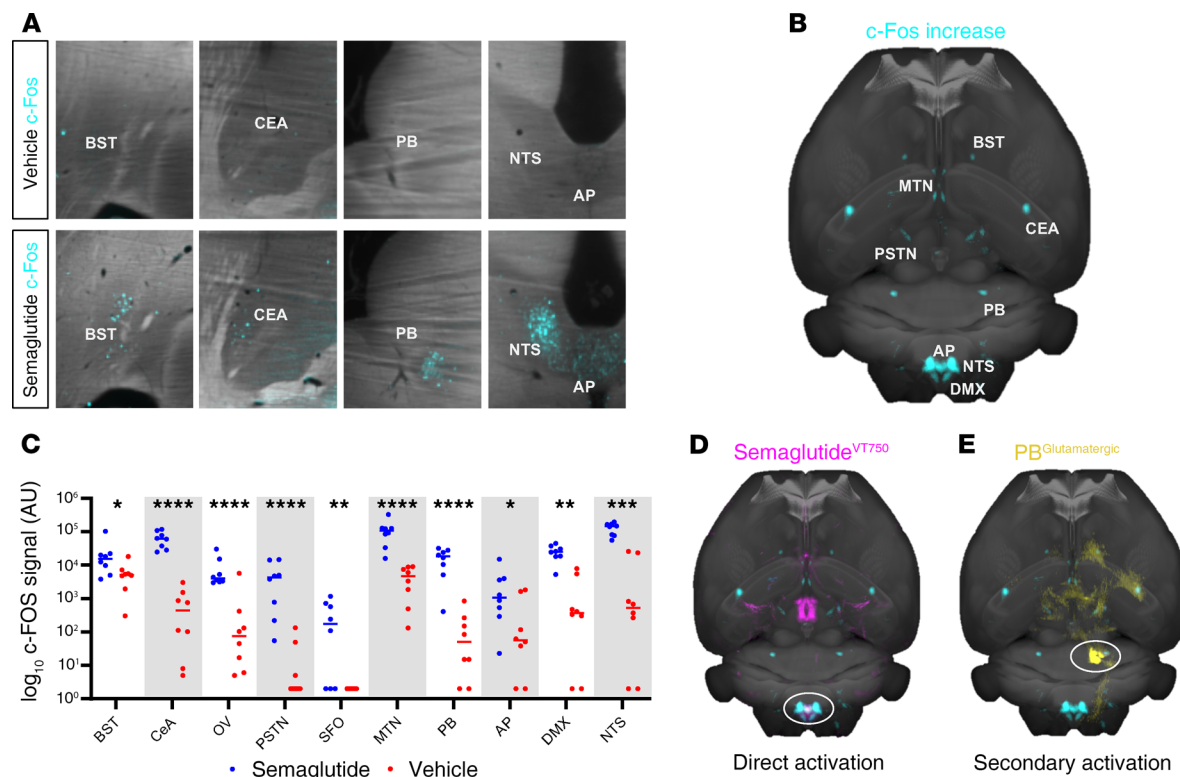


Figure 6. Semaglutide activates a meal termination pathway. (A) c-Fos activation (blue) 4 hours after s.c. semaglutide or vehicle administration (horizontal sections). (B) Horizontal MIP of average c-Fos increase after semaglutide administration ($n = 6$). The signal is overlaid onto the Common Coordinate Framework version 3 template from AIBS. (C) Individual values for c-Fos signal 4 hours after s.c. semaglutide (blue) or vehicle (red) administration. Asterisks indicate enriched regions with FDR of 20%; * $P < 0.05$; ** $P < 0.01$; *** $P < 0.001$; **** $P < 0.0001$. (D) Horizontal MIP of average c-Fos increase (blue) compared with average acute semaglutide VT750 access map (pink). White circle indicates possible direct activation in hindbrain. (E) Horizontal MIP of average c-Fos increase (blue) compared with connectivity map from AIBS outlining unilateral glutamatergic projections from the lateral PB (yellow, PB circled).

median gene expression values. Using these data, an analysis based on Kyoto Encyclopedia of Genes and Genomes (KEGG) pathways was performed to identify overrepresented biological pathways among the DEGs. Figure 7A shows the top 10 overrepresented KEGG pathways.

We observed differences in liraglutide versus weight-matched or vehicle-fed controls, as reflected by significant overrepresentations within a few KEGG pathways (Figure 7A). In contrast, semaglutide appeared to be similar to controls (Figure 7A). Interestingly, differences in KEGG pathway enrichment between the 2 compounds were predominantly observed in the LS, PVH, and ARH, corresponding to the areas with differences in compound distribution. The most significant findings were in the pathways representing ribosomal signaling and oxidative phosphorylation. Figure 7B shows the top 20 differentially regulated genes in these pathways, depicting liraglutide-mediated upregulation in the ARH and downregulation in the PVH and LS, while the expression profile for semaglutide more closely resembled weight-matched and vehicle controls. Supplemental Figure 10D depicts DEGs mapped onto canonical pathways.

An investigation of differences between treatment groups on a single-gene level using transcriptomic data showed noteworthy results for TH. In the ARH, TH was downregulated in the liraglutide group compared with all other groups (Figure 8A, $P < 0.001$, FDR 0.007 liraglutide versus weight-matched control; FDR NS liraglutide versus semaglutide or vehicle control). In the AP, TH was upregulated in both treatment groups compared with vehicle ($P < 0.01$, FDR NS; Figure 8A). A transcriptome analysis of DIO mice treated with the 2 GLP-1RAs for 7 days (BW loss ~18%) showed similar upregulation of TH in the AP, with no differences in the ARH (data not shown). The high degree of TH/GLP-1R overlap in the AP, together with the presence of semaglutide in these neurons (Figure 5), suggests a direct action of the 2 GLP-1RAs on GLP-1R/TH neurons in the AP.

Among the genes differentially expressed in treated versus nontreated rats, prolactin-releasing hormone (PrLH) in the AP represented the most significant finding. PrLH was upregulated about 22-fold in the AP in each treatment group versus vehicle and weight-matched controls (Figure 8B, $P < 0.001$, FDR < 0.001).

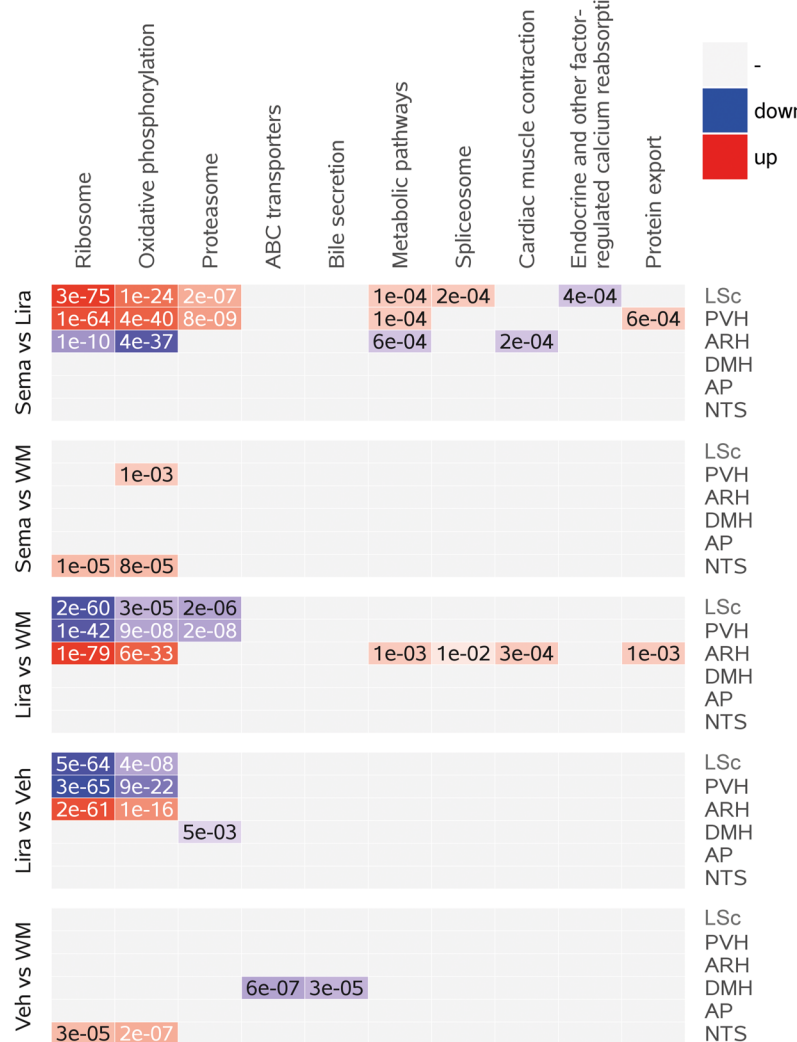
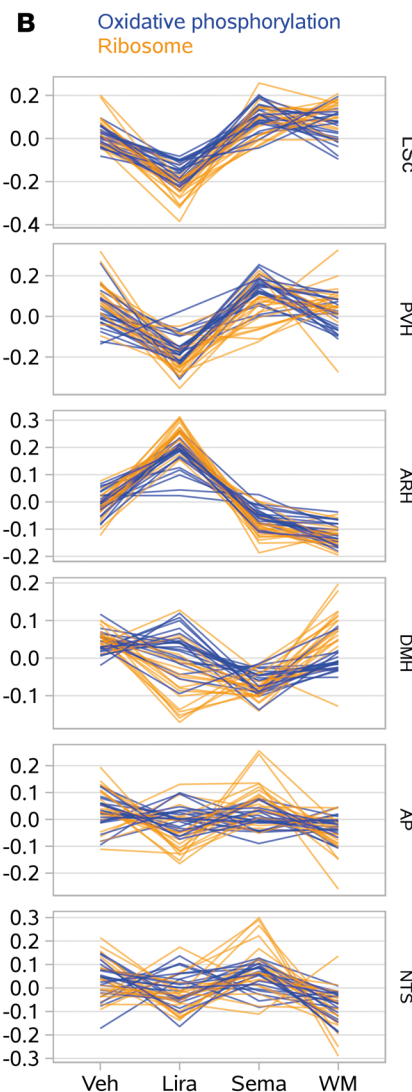
A**B**

Figure 7. Transcriptomic effects across brain regions directly targeted by peripherally administered semaglutide and liraglutide. (A) Top 10 KEGG pathways identified as overrepresented among DEGs (<http://www.genome.jp/kegg/pathway.html>). (B) Line charts of the 2 most highly concordant expression patterns among the DEGs shown in panel A: oxidative phosphorylation (blue) and ribosomal signaling (orange). Each line represents the relative expression of a single gene (median-centered, variance-stabilized expression count across samples for a given tissue/treatment). ABC, ATP-binding cassette; WM, weight matched.

In the NTS, PrLH expression was downregulated approximately 2-fold in the weight-matched group compared with vehicle control ($P < 0.05$, FDR NS). In contrast, downregulation was not observed in either of the GLP-1RA-dosed groups (Figure 8B). This was confirmed in the NTS of mice, whereas no PrLH expression was observed in the AP following treatment with GLP-1RAs (data not shown). IHC for PrRP (product of the PrLH gene) showed that it was upregulated in the AP of rats treated with semaglutide or liraglutide for 7 days, compared with vehicle (Figure 8, C–E). In rats, acute treatment (4 hours) with GLP-1RAs did not increase PrRP levels compared with vehicle (data not shown). Costaining for GLP-1R in the rat AP revealed that all PrRP-positive neurons were GLP-1R positive, whereas not all GLP-1R-positive cells were PrRP positive (Figure 8F). In the NTS, no colocalization was observed between PrRP and GLP-1R. In contrast, although TH exhibited minimal coexpression with PrRP in the AP (Figure 8G), the majority of NTS PrRP-positive neurons also expressed TH (Figure 8H).

Whether PrRP upregulation in the AP was specific to GLP-1RAs was investigated in the AP of DIO rats after receiving vehicle, liraglutide, or a stable amylin analog for 7 days. Only liraglutide induced PrRP expression in the AP (data not shown), suggesting the expression change is specific to GLP-1RA treatment, rather than a general consequence of weight loss.

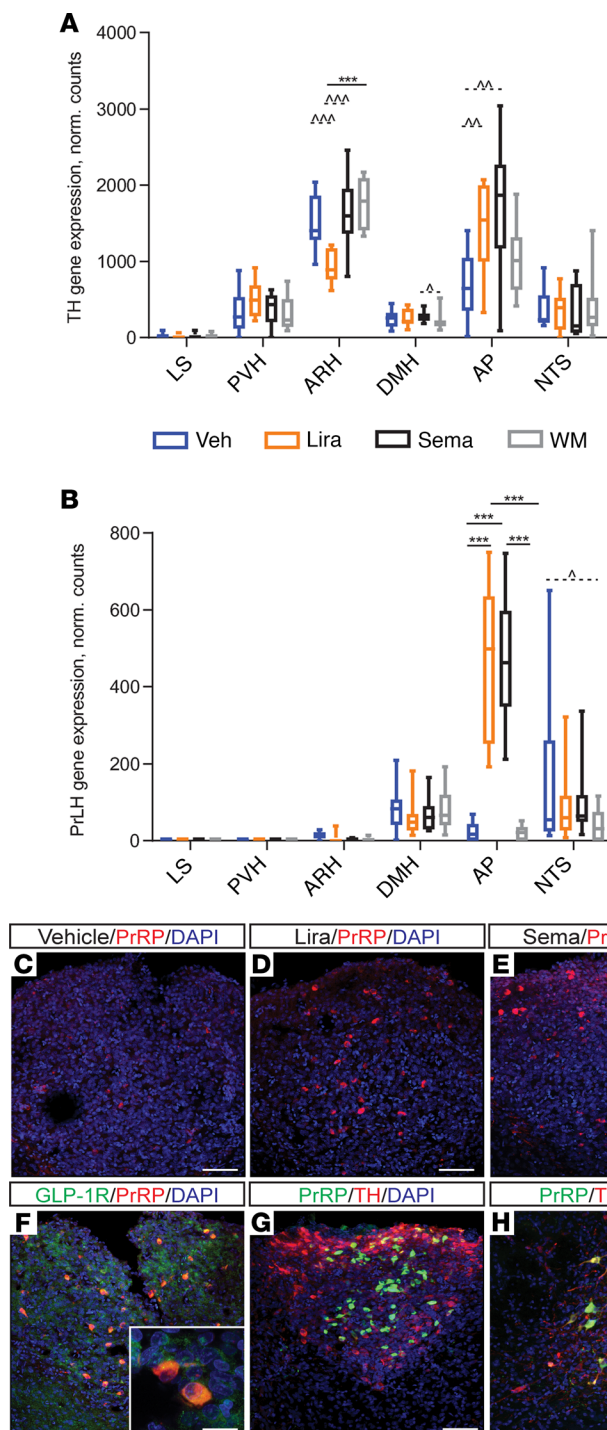


Figure 8. TH and PrLH/PrRP are upregulated in semaglutide-treated rats. Gene expression data for (A) TH and (B) PrLH, shown as box plots with median, interquartile range (box), and max/min (whiskers). *** $P < 0.001$, FDR < 0.05; ^ $P < 0.05$, ^^ $P < 0.01$, and ^^^ $P < 0.001$, FDR > 0.05. (C-H) Representative high-power immunofluorescence images of the AP and NTS stained for PrRP alone, or with GLP-1R or TH, and counterstained with DAPI nuclear stain. PrRP in the AP (C) with vehicle, (D) with liraglutide, (E) with semaglutide, (F) with GLP-1R costaining, (G) with TH costaining, and (H) PrRP and TH in NTS. Scale bars: 10 μ m (E and F insets), 50 μ m (C, D, G and H). PrLH, prolactin-releasing hormone.

Discussion

Numerous studies have investigated the molecular mechanism of GLP-1 in energy homeostasis following direct central administration to select regions of interest with GLP-1R expression. The relatively limited access of peripherally administered liraglutide to the brain (8) has, however, raised the question of which brain regions are relevant for the BW-lowering effects of peripherally administered GLP-1RAs. Here, we show that semaglutide also exhibits limited brain access following peripheral administration, which is unlikely to be driven by general permeation of the BBB. We further identify that semaglutide acts directly on neurons in the hypothalamus and the hindbrain involved in food intake control and, according to whole-brain c-Fos analyses, the pattern of neuronal activation elicited by semaglutide overlaps with neuronal pathways involved in meal termination. We hypothesize that semaglutide may regulate BW by indirect neuronal input to key appetite-modulating relay stations, such as the PB, via several independent brain nuclei that are accessed directly by semaglutide. Finally, the transcriptomic profile in brain regions directly targeted by semaglutide was evaluated and revealed potentially novel GLP-1RA-regulated genes, such as PrLH.

Previous studies have demonstrated that i.v. GLP-1 and exendin-4 can enter the brain (34), and it has been widely assumed that GLP-1 and related peptides cross the BBB. However, several observations do not support general BBB permeability, including the limited brain access observed with fluorescently labeled semaglutide in the present study, together with analogous results with GLP-1 (35) and liraglutide (8). The in vitro BBB model used here substantiated this, and we did not find GLP-1R expression in endothelial cells using electron microscopy, whereas expression in tanycytes lining the third ventricular wall of the ventromedial ARH was found.

Studies describe distinct populations of tanycytes around the third ventricle, which display significantly different gene expression patterns (36). The role of GLP-1Rs on tanycytes remains to be fully characterized, but they may be involved in transport of semaglutide into the ARH. This population of tanycytes could also serve as neuro and glial progenitor cells (36) and has been implicated in glucose sensing because a fraction of tanycytes extend down to the ME, where their end-feet contact permeable fenestrated vessels (37).

Semaglutide exhibited potent BW-lowering effects in rodents. Although the primary driver of semaglutide-induced weight loss was reduced food intake, additional effects were observed. Of note, by the end of an 11-day period, EE in control mice weight-matched to the semaglutide group by food restriction was reduced, whereas EE in the semaglutide-treated group returned to baseline levels. This suggests that

semaglutide maintains metabolic activity (or prevents compensatory downregulation of EE) despite weight loss, thereby aiding in prolonged weight loss or maintenance. Clinically, minor reductions in EE have been observed in patients receiving liraglutide or semaglutide compared with placebo (1, 6). This was not significant when adjusting for lean body mass. However, in clinical studies EE was measured during active weight loss, whereas in our studies EE was measured at plateau; it is possible, therefore, that at steady state semaglutide may have a small effect on preventing further reduction in EE in patients.

Semaglutide influenced palatable food consumption by shifting food preference away from chocolate, also observed previously in rats receiving liraglutide (38, 39). These results are in accordance with observations in humans where reward and food preference were altered in response to GLP-1RA treatment, including semaglutide (6, 40–43). Although these clinical and animal studies (21–25, 44–49) indicate that several brain regions are involved in GLP-1RA-regulated reward behaviors, the exact mechanisms remain unclear. Data suggest the involvement of dopamine release from the VTA (44, 47, 50). Projections have been mapped between the VTA and LSc (51), and acute stimulation of GLP-1Rs in the LSc leads to enhanced LSc dopamine transporter surface expression and function. It has been suggested that this effect is mediated by a reduction in endocannabinoid and arachidonic acid levels in the LSc and decreased synaptic dopamine levels (44). Furthermore, direct LSc GLP-1R stimulation suppresses food intake and motivation for food in rats (52). In the current study, fluorescently labeled semaglutide was detected in the LSc, allowing for the possibility of similar reductions in dopamine levels in this region (44) and an ability to influence food intake and motivation. Only fluorescently labeled semaglutide, and not liraglutide, was observed in the LSc following peripheral administration. Because this was apparent following acute and steady-state administration, differences in plasma half-lives alone do not explain this difference. Despite the direct targeting of semaglutide to the LSc, no c-Fos-related neuronal activation was observed in the LSc following semaglutide administration. Quantitatively, the LSc represents an area with some of the highest numbers of GLP-1Rs (12, 53), but here the GLP-1R expression is predominantly on neuronal projections, which could explain the lack of activation in this region. Alternatively, semaglutide could inhibit neurons in this area. No direct comparison has been made between semaglutide and liraglutide on food preference in preclinical studies, and it remains to be determined whether differential access to the LSc translates into clinical differences in food preference.

The pathway analyses of the transcriptome data revealed differential regulation of pathways, including ribosomal (eukaryotic initiation factor 2 and 4 signaling) and mitochondrial (oxidative phosphorylation), between liraglutide- and semaglutide-treated animals. These differences could be driven by direct GLP-1R activation or indirect factors; for instance, insulin is the prototypical regulator of the initiation factor signaling pathway through PI3K activation (54). Thus, the differential regulation of the oxidative phosphorylation pathway could reflect improved insulin sensitivity in response to increased insulin-driven ROS production, which has been suggested to inhibit food intake via the hypothalamus (55, 56). Interestingly, under hypoxic conditions, GLP-1R stimulation by liraglutide reduces the generation of ROS (57). Overall, semaglutide-treated animals exhibited expression patterns that were closer to the weight-matched group, particularly in the ARH and LSc. These areas correspond to regional distribution differences between semaglutide and liraglutide, which may explain the discrepancies between the 2 GLP-1RAs by virtue of differences in GLP-1R interaction in these specific brain regions.

Among the DEGs identified, the most significant finding was upregulation of PrLH in the AP following liraglutide or semaglutide administration, which translated into upregulation of PrRP at the protein level (Figure 8). We established that this is likely a consequence of GLP-1RA treatment, rather than a general change associated with weight loss, because it was not evident with other agents (amylin) yielding similar weight loss and did not occur in the weight-matched group. PrRP delivery to the NTS at the level of the AP decreases BW, food intake, and meal size in rats (58). This suggests an inducible system of PrRP production triggered by GLP-1RAs. Given that all PrRP-positive neurons in the AP also expressed GLP-1Rs, it is conceivable that PrRP production is driven through direct activation of the GLP-1Rs in this nucleus. In the NTS, PrLH mRNA expression was downregulated exclusively by weight loss caused by food restriction, as shown previously (59, 60). The observed expression pattern of PrLH varied between DIO rats and DIO mice; only rats showed induction of PrLH in the AP after GLP-1RA administration, whereas the expression patterns in the NTS were similar for both species. Discrepancies between PrRP neurons in mice and rats have also been reported in the literature; for example, NTS PrRP neurons are leptin sensitive in rats but not in mice (61). PrRP is putatively involved in neuroendocrine function, including energy homeostasis,

stress response, cardiovascular regulation, and circadian function (62), and it has been reported to lower BW in rodents, potentially through regulation of food intake and EE (62). Liraglutide reduces food intake (although dose independently) in Otsuka Long-Evans Tokushima Fatty rats harboring a natural mutation in the PrRP receptor (63). Furthermore, we have previously shown that liraglutide can still reduce BW after AP ablation (8). Based on these data and our observations, we hypothesize that PrRP in the hindbrain could be one of several mechanisms involved in the BW-lowering effects of GLP-1RAs, although it is not strictly required. Of note, TH gene expression was substantially upregulated in the AP following GLP-1RA administration (Figure 8A), as demonstrated previously using complementary methods (64). The majority of TH-positive neurons expressed GLP-1R, but in the AP only a limited number of PrRP-positive neurons also expressed TH, suggesting activation of different cell populations expressing the GLP-1R in AP. Where TH overlapped extensively with the GLP-1R-expressing neurons in the AP, fluorescently labeled semaglutide was highly abundant. Limited overlap exists between TH and the vesicular glutamate transporter (data not shown); thus, in the AP, TH-positive cells are likely the A1 cell group that produces norepinephrine (NE). These project to adjacent A2 cells in the NTS and are involved in the decreased food intake associated with anorexic agents such as lithium chloride and cholecystokinin (65, 66).

Fluorescently labeled semaglutide was seen in regions classically associated with GLP-1R-mediated regulation of food intake, such as the hypothalamic ARH and the AP and NTS in the brainstem. The ARH is involved in mediating liraglutide-regulated food intake and weight loss through direct activation of POMC/CART and indirect inhibition of NPY/AgRP neurons (8, 14). In the current study, these findings were confirmed by direct semaglutide-stimulated activation of POMC neurons and inhibition of NPY neurons in electrophysiological current clamp recordings. These data support the gene expression data that showed upregulation of CART mRNA in the ARH following semaglutide administration, with simultaneous attenuation of hunger-stimulated increases in NPY and AgRP mRNA levels that were observed in the weight-matched controls. This suggests a direct interaction between semaglutide and GLP-1Rs in ARH, further substantiated by the accumulation of labeled semaglutide in CART-positive cells in this region.

Semaglutide was also seen in a small population of TH- and GLP-1R-positive cells in the ARH. TH is the rate-limiting enzyme for catecholamine synthesis, leading to dopamine and NE production, and because the ARH lacks the NE-converting enzyme dopamine β -hydroxylase, the TH-positive cells in this region are believed to be of a dopaminergic nature. Limited data exist regarding ARH dopamine effects on food intake, but one study reported increased food intake following stimulation of dopamine neurons in the ARH (67). TH-positive neurons in the ARH have been considered a relatively uniform population of tuberoinfundibular dopamine neurons, involved in the regulation of prolactin release through dopamine secretion to the ME (68). Emerging literature suggests, however, that this population is heterogeneous, with local synaptic inhibitory GABAergic projections to other ARH neurons (27, 29, 69, 70). In rats, TH mRNA was downregulated in ARH following liraglutide treatment. The impact of decreased TH expression on food intake, and its translational relevance, remain speculative because the effect was not observed in mice. Of note, the dopamine neurons in the ARH also regulate pituitary hormones (71), which could be linked to the GLP-1 stimulatory release of pituitary hormones, such as vasopressin and corticotropin-releasing hormone (72).

In the ARH, a large proportion of SST-expressing cells coexpressed GLP-1R. SST is associated with the inhibition of growth hormone (73) and a range of extrapituitary effects, including body temperature and visceral functions (74–77). When delivered centrally, SST increases food intake (78, 79). This divergence in functionality between SST and the anorexigenic effects of GLP-1RAs would appear to exclude the involvement of SST in the regulation of appetite by semaglutide. However, the respiratory quotient has also been reported to be increased by central SST actions independent of the orexigenic effects (80). Conceivably, this effect of SST may, in part, explain the sustained EE observed in the semaglutide-treated mice despite weight loss.

It has been suggested that other regions, such as the ACB, LHA, MTN/PVT, and VTA, could mediate the regulatory effect of GLP-1RAs on food intake (21–25). Studies suggest a role for brain-derived GLP-1 in the control of eating and reward (80, 81), but there is no evidence that peripherally administered GLP-1RAs can directly access GLP-1Rs in these regions, as demonstrated by the lack of fluorescently labeled semaglutide in these brain nuclei. Thus, activation of brain-derived GLP-1 would be necessary for peripherally circulating GLP-1/GLP-1RAs to engage GLP-1Rs in regions such as the ACB or VTA. Furthermore, this engagement is likely to be indirect because expression of GLP-1Rs on NTS GLP-1-producing cells has not been documented (82). We previously compared the c-Fos activation pattern in NTS preproglu-

gon (PPG) neurons following liraglutide administration with that induced by food restriction. Both food restriction and liraglutide induced c-Fos in the NTS; however, only food restriction induced c-Fos in PPG neurons, suggesting that peripherally circulating GLP-1RAs do not activate PPG neurons in the NTS (83). Downregulation of PPG mRNA levels by chronic GLP-1RA administration and food restriction in rats (8) further substantiates these findings. Thus, we suggest that the majority of GLP-1R regions in the CNS are likely targets for brain-derived GLP-1 rather than exogenously administered GLP-1RAs.

Whole-brain c-Fos staining revealed that semaglutide activated 10 brain nuclei, and an overlap between c-Fos signaling and fluorescently labeled semaglutide was observed only in the AP, NTS, and DMX in the brainstem. Comparing c-Fos signals and AIBS connectivity maps revealed that the c-Fos activation observed in several regions (CeA, MTN/PVT, and BST) correlated with projections from the lateral PB, as exemplified by the glutamatergic cells in the PB (SLC17A6). The c-Fos activation patterns in the AP, NTS, PB, and CeA are well described for other appetite-modulating compounds, including glucagon (84), lithium chloride (85–87), amylin (87), and GLP-1 (18). Direct innervation of the PB by neurons originating in the NTS and AP in the brainstem and in the hypothalamic ARH have been demonstrated (88, 89), suggesting an activation pathway for endogenous blood-borne hormones, such as leptin (27), ghrelin (90), and GLP-1 (8), that affects PB signaling. The PB is an important nucleus for appetite and blood glucose modulation, conveying information from the brainstem to the CeA and BST (31, 91, 92). Consequently, it has been suggested that the PB serves as a key integrator of hypothalamic energy homeostasis signals with visceral and gustatory information from the brainstem (32, 93). Within the PB, the CGRP-positive cells are essential in food intake regulation and are involved in GLP-1-related effects on BW (31, 91). A population of cells in the dI PB were both CGRP positive and c-Fos positive following semaglutide administration. Thus, the observed c-Fos activation pattern elicited by semaglutide in this study is consistent with a brainstem-to-amygdala circuit engaged in appetite-regulating pathways. Interestingly, a discrete population of c-Fos-positive cells in the dI PB were not CGRP positive, indicating that other neurons in the PB are activated by GLP-1RA administration. The PB is largely innervated by glutamatergic neurons from the AP and NTS. GLP-1Rs in the AP overlapped with the vesicular glutamate transporter, whereas there was a lack of GLP-1R-positive cell bodies in the NTS, suggesting that the entry point for GLP-1RAs could be through AP directly innervating PB. An earlier study showed that AP neurons project extensively to the dI part of the PB (94), the region with c-Fos activation in CGRP-positive neurons in the current study. Therefore, indirect stimulation of the PB via the NTS following afferent stimulation from GLP-1R-/TH-positive neurons in AP is plausible.

Inhibition of the PB by hypothalamic AgRP neurons is involved in the regulation of food intake (31, 95–97): silencing AgRP neurons elicits a robust PB c-Fos response, leading to starvation of animals and ultimately death (96, 98). POMC neurons also project to the PB (99, 100). In tandem, both innervation pathways can modulate the PB by fine-tuning downstream signaling from the PB. Electrophysiological recordings showed that semaglutide activated POMC neurons directly in the ARH, which could mediate additional activation of PB. NPY neurons, also known to express AgRP, were inhibited by semaglutide, suggesting disinhibition of AgRP signaling to the PB, resulting in increased activation of this nucleus. These data support direct modulation of PB signaling by semaglutide-induced neuronal stimulation in the hypothalamus. Only the medial and posterior parts of ARH AgRP neurons project to the PB (95), and clinical studies have identified the posterior region of the hypothalamus as having a crucial effect on BW (101, 102). This finding could be relevant, considering that semaglutide, but not liraglutide, is present in the posterior ARH and could therefore further modulate AgRP input to the PB. Although limited evidence exists for GLP-1R expression on AgRP neurons, electrophysiological recordings demonstrated that indirect modulation is achievable (8). Finally, a basal-forebrain AgRP circuit has been identified, whereby AgRP elicits increased food intake through projections directly to the BST (95). The proposed modulation of the PB, via indirect inhibition of AgRP by GLP-1, could also aid in the modulation of the BST by removing AgRP-mediated inhibition of this nucleus, thereby enabling — and potentially enhancing — the appetite-reducing PB-to-BST pathway. In Supplemental Figure 11, we hypothesize how semaglutide may regulate BW by affecting neuronal input to the PB from several independent brain nuclei, including the AP and ARH, both direct targets of semaglutide.

To conclude, we have shown that the GLP-1RA semaglutide reduces BW through direct effects in the hypothalamus and the hindbrain as well as secondary effects in several areas previously described to be involved in energy metabolism.

Methods

Please see Supplemental Methods. RNA-Seq data have been deposited into the ArrayExpress database (<http://www.ebi.ac.uk/arrayexpress>) under accession number E-MTAB-8078.

Study approval. All animal studies were conducted in compliance with internationally accepted principles for the care and use of laboratory animals and were approved by the internal Novo Nordisk Ethical Review Committee in Denmark. Studies performed in Denmark were conducted according to approved national regulations and with animal experimental licenses granted by the Danish Ministry of Justice. In addition to internal Novo Nordisk approval and compliance with international standards for animal care and use, the DIO mouse study (Figure 1, A and B) performed at Novo Nordisk, China, was conducted under licenses granted by the Beijing Administration Office of Laboratory Animals. Animal studies for electron microscopy were approved by the Animal Welfare Committees at the Institute of Experimental Medicine of the Hungarian Academy of Sciences.

Author contributions

SG, CGS, SJP, JAR, TA, AFB, STB, EF, CF, KSF, HCCH, JFP, LMJ, CP, JN, TTL, JPW, VP, KR, LS, GS, ASS, HW, AS, and LBK were involved in designing, calculating, or carrying out experiments; preparing figures; and writing the methods section for the manuscript. The main part of the manuscript was written by SG, SJP, KSF, JPW, AS, and LBK. WFJH designed and synthesized all fluorescently labelled peptides used in the studies, and contributed to discussions of study designs and data.

Acknowledgments

The following technicians are thanked: Elena Carlsen, Hanife D. Farizi, Jeanette Bannebjerg Johansen, Sanne L. Maribo, Heidi Solvang Nielsen, Maria Bjerremann Rasmussen, and Frank Strauss. We thank AXON Communications for editorial assistance, funded by Novo Nordisk.

Address correspondence to: Lotte Bjerre Knudsen, Novo Nordisk, Novo Nordisk Park, DK-2700 Måløv, Denmark. Phone: 45.30754788; Email: lbkn@novonordisk.com.

SG's present address is: Lund University, Lund, Sweden.

CGS's present address is: Gubra, Hørsholm, Denmark.

TA's present address is: Umea University, Umea, Sweden.

HCCH and JN's present address is: University of Copenhagen, Copenhagen, Denmark.

GS's present address is: Pegbio, Jiangsu Province, China.

1. van Can J, Sloth B, Jensen CB, Flint A, Blaak EE, Saris WH. Effects of the once-daily GLP-1 analog liraglutide on gastric emptying, glycemic parameters, appetite and energy metabolism in obese, non-diabetic adults. *Int J Obes (Lond)*. 2014;38(6):784–793.
2. Lau J, et al. Discovery of the once-weekly glucagon-like peptide-1 (GLP-1) analogue semaglutide. *J Med Chem*. 2015;58(18):7370–7380.
3. Pratley RE, et al. Semaglutide versus dulaglutide once weekly in patients with type 2 diabetes (SUSTAIN 7): a randomised, open-label, phase 3b trial. *Lancet Diabetes Endocrinol*. 2018;6(4):275–286.
4. Ahmann AJ, et al. Efficacy and safety of once-weekly semaglutide versus exenatide ER in subjects with type 2 diabetes (SUSTAIN 3): a 56-week, open-label, randomized clinical trial. *Diabetes Care*. 2018;41(2):258–266.
5. O'Neil PM, et al. Efficacy and safety of semaglutide compared with liraglutide and placebo for weight loss in patients with obesity: a randomised, double-blind, placebo and active controlled, dose-ranging, phase 2 trial. *Lancet*. 2018;392(10148):637–649.
6. Blundell J, et al. Effects of once-weekly semaglutide on appetite, energy intake, control of eating, food preference and body weight in subjects with obesity. *Diabetes Obes Metab*. 2017;19(9):1242–1251.
7. Marso SP, Holst AG, Vilsbøll T. Semaglutide and cardiovascular outcomes in patients with type 2 diabetes. *N Engl J Med*. 2017;376(9):891–892.
8. Secher A, et al. The arcuate nucleus mediates GLP-1 receptor agonist liraglutide-dependent weight loss. *J Clin Invest*. 2014;124(10):4473–4488.
9. Sisley S, Gutierrez-Aguilar R, Scott M, D'Alessio DA, Sandoval DA, Seeley RJ. Neuronal GLP1R mediates liraglutide's anorectic but not glucose-lowering effect. *J Clin Invest*. 2014;124(6):2456–2463.
10. Göke R, Larsen PJ, Mikkelsen JD, Sheikh SP. Distribution of GLP-1 binding sites in the rat brain: evidence that exendin-4 is a

- ligand of brain GLP-1 binding sites. *Eur J Neurosci*. 1995;7(11):2294–2300.
11. Heppner KM, et al. Expression and distribution of glucagon-like peptide-1 receptor mRNA, protein and binding in the male nonhuman primate (*Macaca mulatta*) brain. *Endocrinology*. 2015;156(1):255–267.
 12. Jensen CB, Pyke C, Rasch MG, Dahl AB, Knudsen LB, Secher A. Characterization of the glucagonlike peptide-1 receptor in male mouse brain using a novel antibody and *in situ* hybridization. *Endocrinology*. 2018;159(2):665–675.
 13. Turton MD, et al. A role for glucagon-like peptide-1 in the central regulation of feeding. *Nature*. 1996;379(6560):69–72.
 14. Barreto-Viana AR, Aguil MB, Mandarim-de-Lacerda CA. Effects of liraglutide in hypothalamic arcuate nucleus of obese mice. *Obesity (Silver Spring)*. 2016;24(3):626–633.
 15. Hayes MR, Bradley L, Grill HJ. Endogenous hindbrain glucagon-like peptide-1 receptor activation contributes to the control of food intake by mediating gastric satiation signaling. *Endocrinology*. 2009;150(6):2654–2659.
 16. Hayes MR, Skibicka KP, Grill HJ. Caudal brainstem processing is sufficient for behavioral, sympathetic, and parasympathetic responses driven by peripheral and hindbrain glucagon-like-peptide-1 receptor stimulation. *Endocrinology*. 2008;149(8):4059–4068.
 17. Kinzig KP, D’Alessio DA, Seeley RJ. The diverse roles of specific GLP-1 receptors in the control of food intake and the response to visceral illness. *J Neurosci*. 2002;22(23):10470–10476.
 18. Swick JC, et al. Parabrachial nucleus contributions to glucagon-like peptide-1 receptor agonist-induced hypophagia. *Neuropsychopharmacology*. 2015;40(8):2001–2014.
 19. Adams JM, et al. Liraglutide modulates appetite and body weight through glucagon-like peptide 1 receptor-expressing glutamatergic neurons. *Diabetes*. 2018;67(8):1538–1548.
 20. Burmeister MA, et al. The hypothalamic glucagon-like peptide 1 receptor is sufficient but not necessary for the regulation of energy balance and glucose homeostasis in mice. *Diabetes*. 2017;66(2):372–384.
 21. Alhadeff AL, Rupprecht LE, Hayes MR. GLP-1 neurons in the nucleus of the solitary tract project directly to the ventral tegmental area and nucleus accumbens to control for food intake. *Endocrinology*. 2012;153(2):647–658.
 22. Mietlicki-Baase EG, et al. Glucagon-like peptide-1 receptor activation in the nucleus accumbens core suppresses feeding by increasing glutamatergic AMPA/kainate signaling. *J Neurosci*. 2014;34(20):6985–6992.
 23. Mietlicki-Baase EG, et al. The food intake-suppressive effects of glucagon-like peptide-1 receptor signaling in the ventral tegmental area are mediated by AMPA/kainate receptors. *Am J Physiol Endocrinol Metab*. 2013;305(11):E1367–E1374.
 24. Ong ZY, Liu JJ, Pang ZP, Grill HJ. Paraventricular thalamic control of food intake and reward: role of glucagon-like peptide-1 receptor signaling. *Neuropsychopharmacology*. 2017;42(12):2387–2397.
 25. López-Ferreras L, et al. Lateral hypothalamic GLP-1 receptors are critical for the control of food reinforcement, ingestive behavior and body weight. *Mol Psychiatry*. 2018;23(5):1157–1168.
 26. Helms HC, et al. In vitro models of the blood-brain barrier: An overview of commonly used brain endothelial cell culture models and guidelines for their use. *J Cereb Blood Flow Metab*. 2016;36(5):862–890.
 27. Balland E, et al. Hypothalamic tanycytes are an ERK-gated conduit for leptin into the brain. *Cell Metab*. 2014;19(2):293–301.
 28. Prevot V, Cornea A, Mungenast A, Smiley G, Ojeda SR. Activation of erbB-1 signaling in tanycytes of the median eminence stimulates transforming growth factor beta1 release via prostaglandin E2 production and induces cell plasticity. *J Neurosci*. 2003;23(33):10622–10632.
 29. Zhang X, van den Pol AN. Dopamine/tyrosine hydroxylase neurons of the hypothalamic arcuate nucleus release GABA, communicate with dopaminergic and other arcuate neurons, and respond to dynorphin, met-enkephalin, and oxytocin. *J Neurosci*. 2015;35(45):14966–14982.
 30. Cai H, Haubensal W, Anthony TE, Anderson DJ. Central amygdala PKC-δ(+) neurons mediate the influence of multiple anorexigenic signals. *Nat Neurosci*. 2014;17(9):1240–1248.
 31. Campos CA, Bowen AJ, Schwartz MW, Palmiter RD. Parabrachial CGRP neurons control meal termination. *Cell Metab*. 2016;23(5):811–820.
 32. Carter ME, Soden ME, Zweifel LS, Palmiter RD. Genetic identification of a neural circuit that suppresses appetite. *Nature*. 2013;503(7474):111–114.
 33. Roman CW, Derkach VA, Palmiter RD. Genetically and functionally defined NTS to PBN brain circuits mediating anorexia. *Nat Commun*. 2016;7:11905.
 34. Kastin AJ, Akerstrom V, Pan W. Interactions of glucagon-like peptide-1 (GLP-1) with the blood-brain barrier. *J Mol Neurosci*. 2002;18(1-2):7–14.
 35. Orskov C, Poulsen SS, Møller M, Holst JJ. Glucagon-like peptide I receptors in the subfornical organ and the area postrema are accessible to circulating glucagon-like peptide I. *Diabetes*. 1996;45(6):832–835.
 36. Campbell JN, et al. A molecular census of arcuate hypothalamus and median eminence cell types. *Nat Neurosci*. 2017;20(3):484–496.
 37. Prevot V, Dehouck B, Sharif A, Ciofi P, Giacobini P, Clasadonte J. The versatile tanycyte: a hypothalamic integrator of reproduction and energy metabolism. *Endocr Rev*. 2018;39(3):333–368.
 38. Hansen G, Jelsing J, Vrang N. Effects of liraglutide and sibutramine on food intake, palatability, body weight and glucose tolerance in the guinea pig DIO-rats. *Acta Pharmacol Sin*. 2012;33(2):194–200.
 39. Raun K, von Voss P, Gotfredsen CF, Golozoubova V, Rolin B, Knudsen LB. Liraglutide, a long-acting glucagon-like peptide-1 analog, reduces body weight and food intake in obese candy-fed rats, whereas a dipeptidyl peptidase-IV inhibitor, vildagliptin, does not. *Diabetes*. 2007;56(1):8–15.
 40. Farr OM, et al. GLP-1 receptors exist in the parietal cortex, hypothalamus and medulla of human brains and the GLP-1 analogue liraglutide alters brain activity related to highly desirable food cues in individuals with diabetes: a crossover, randomised, placebo-controlled trial. *Diabetologia*. 2016;59(5):954–965.
 41. Inoue K, et al. Short-term effects of liraglutide on visceral fat adiposity, appetite, and food preference: a pilot study of obese Japanese patients with type 2 diabetes. *Cardiovasc Diabetol*. 2011;10:109.
 42. van Bloemendaal L, et al. GLP-1 receptor activation modulates appetite- and reward-related brain areas in humans. *Diabetes*. 2014;63(12):4186–4196.
 43. van Bloemendaal L, et al. Brain reward-system activation in response to anticipation and consumption of palatable food is altered by glucagon-like peptide-1 receptor activation in humans. *Diabetes Obes Metab*. 2015;17(9):878–886.

44. Reddy IA, et al. Glucagon-like peptide 1 receptor activation regulates cocaine actions and dopamine homeostasis in the lateral septum by decreasing arachidonic acid levels. *Transl Psychiatry*. 2016;6:e809.
45. Richard JE, Anderberg RH, Göteson A, Gribble FM, Reimann F, Skibicka KP. Activation of the GLP-1 receptors in the nucleus of the solitary tract reduces food reward behavior and targets the mesolimbic system. *PLoS One*. 2015;10(3):e0119034.
46. Schmidt HD, et al. Glucagon-Like peptide-1 receptor activation in the ventral tegmental area decreases the reinforcing efficacy of cocaine. *Neuropsychopharmacology*. 2016;41(7):1917–1928.
47. Harasta AE, et al. Septal glucagon-like peptide 1 receptor expression determines suppression of cocaine-induced behavior. *Neuropsychopharmacology*. 2015;40(8):1969–1978.
48. Tuesta LM, et al. GLP-1 acts on habenular avoidance circuits to control nicotine intake. *Nat Neurosci*. 2017;20(5):708–716.
49. Dossat AM, Diaz R, Gallo L, Panagos A, Kay K, Williams DL. Nucleus accumbens GLP-1 receptors influence meal size and palatability. *Am J Physiol Endocrinol Metab*. 2013;304(12):E1314–E1320.
50. Dickson SL, Shirazi RH, Hansson C, Bergquist F, Nissbrant H, Skibicka KP. The glucagon-like peptide 1 (GLP-1) analogue, exendin-4, decreases the rewarding value of food: a new role for mesolimbic GLP-1 receptors. *J Neurosci*. 2012;32(14):4812–4820.
51. Luo AH, Tahsili-Fahadan P, Wise RA, Lupica CR, Aston-Jones G. Linking context with reward: a functional circuit from hippocampal CA3 to ventral tegmental area. *Science*. 2011;333(6040):353–357.
52. Terrill SJ, et al. Role of lateral septum glucagon-like peptide 1 receptors in food intake. *Am J Physiol Regul Integr Comp Physiol*. 2016;311(1):R124–R132.
53. Cork SC, Richards JE, Holt MK, Gribble FM, Reimann F, Trapp S. Distribution and characterisation of Glucagon-like peptide-1 receptor expressing cells in the mouse brain. *Mol Metab*. 2015;4(10):718–731.
54. Proud CG. Regulation of protein synthesis by insulin. *Biochem Soc Trans*. 2006;34(Pt 2):213–216.
55. Storozhevych TP, Senilova YE, Persiyantseva NA, Pinelis VG, Pomytkin IA. Mitochondrial respiratory chain is involved in insulin-stimulated hydrogen peroxide production and plays an integral role in insulin receptor autophosphorylation in neurons. *BMC Neurosci*. 2007;8:84.
56. Drougard A, Fournel A, Valet P, Knauf C. Impact of hypothalamic reactive oxygen species in the regulation of energy metabolism and food intake. *Front Neurosci*. 2015;9:56.
57. Zhu H, et al. The neuroprotection of liraglutide against ischaemia-induced apoptosis through the activation of the PI3K/AKT and MAPK pathways. *Sci Rep*. 2016;6:26859.
58. Davis XS, Grill HJ. The hindbrain is a site of energy balance action for prolactin-releasing peptide: feeding and thermic effects from GPR10 stimulation of the nucleus tractus solitarius/area postrema. *Psychopharmacology (Berl)*. 2018;235(8):2287–2301.
59. Lawrence CB, Celsi F, Brennan J, Luckman SM. Alternative role for prolactin-releasing peptide in the regulation of food intake. *Nat Neurosci*. 2000;3(7):645–646.
60. Dodd GT, et al. The thermogenic effect of leptin is dependent on a distinct population of prolactin-releasing peptide neurons in the dorsomedial hypothalamus. *Cell Metab*. 2014;20(4):639–649.
61. Maniscalco JW, Kreisler AD, Rinaman L. Satiation and stress-induced hypophagia: examining the role of hindbrain neurons expressing prolactin-releasing Peptide or glucagon-like Peptide 1. *Front Neurosci*. 2012;6:199.
62. Dodd GT, Luckman SM. Physiological roles of GPR10 and PrRP signaling. *Front Endocrinol (Lausanne)*. 2013;4:20.
63. Guo N, Sun J, Chen H, Zhang H, Zhang Z, Cai D. Liraglutide prevents diabetes progression in prediabetic OLETF rats. *Endocr J*. 2013;60(1):15–28.
64. Yamamoto H, et al. Glucagon-like peptide-1-responsive catecholamine neurons in the area postrema link peripheral glucagon-like peptide-1 with central autonomic control sites. *J Neurosci*. 2003;23(7):2939–2946.
65. Rinaman L. Hindbrain noradrenergic A2 neurons: diverse roles in autonomic, endocrine, cognitive, and behavioral functions. *Am J Physiol Regul Integr Comp Physiol*. 2011;300(2):R222–R235.
66. Cunningham ET, Miselis RR, Sawchenko PE. The relationship of efferent projections from the area postrema to vagal motor and brain stem catecholamine-containing cell groups: an axonal transport and immunohistochemical study in the rat. *Neuroscience*. 1994;58(3):635–648.
67. Zhang X, van den Pol AN. Hypothalamic arcuate nucleus tyrosine hydroxylase neurons play orexigenic role in energy homeostasis. *Nat Neurosci*. 2016;19(10):1341–1347.
68. Tuomisto J, Männistö P. Neurotransmitter regulation of anterior pituitary hormones. *Pharmacol Rev*. 1985;37(3):249–332.
69. Björklund A, Dunnett SB. Fifty years of dopamine research. *Trends Neurosci*. 2007;30(5):185–187.
70. Brown RS, et al. Conditional deletion of the prolactin receptor reveals functional subpopulations of dopamine neurons in the arcuate nucleus of the hypothalamus. *J Neurosci*. 2016;36(35):9173–9185.
71. Baik JH. Dopamine signaling in food addiction: role of dopamine D2 receptors. *BMB Rep*. 2013;46(11):519–526.
72. Larsen PJ, Tang-Christensen M, Jessop DS. Central administration of glucagon-like peptide-1 activates hypothalamic neuroendocrine neurons in the rat. *Endocrinology*. 1997;138(10):4445–4455.
73. Brazeau P, et al. Hypothalamic polypeptide that inhibits the secretion of immunoreactive pituitary growth hormone. *Science*. 1973;179(4068):77–79.
74. Brown M, Taché Y. Hypothalamic peptides: central nervous system control of visceral functions. *Fed Proc*. 1981;40(11):2565–2569.
75. Brown MR. Somatostatin-28 effects on central nervous system regulation of vasopressin secretion and blood pressure. *Neuroendocrinology*. 1988;47(6):556–562.
76. Hajdu I, Obál F, Gardi J, Lacz I, Krueger JM. Octreotide-induced drinking, vasopressin, and pressure responses: role of central angiotensin and ACh. *Am J Physiol Regul Integr Comp Physiol*. 2000;279(1):R271–R277.
77. Stengel A, Karasawa H, Taché Y. The role of brain somatostatin receptor 2 in the regulation of feeding and drinking behavior. *Horm Behav*. 2015;73:15–22.
78. Stengel A, et al. Central injection of the stable somatostatin analog ODT8-SST induces a somatostatin2 receptor-mediated orexigenic effect: role of neuropeptide Y and opioid signaling pathways in rats. *Endocrinology*. 2010;151(9):4224–4235.
79. Karasawa H, Yakabi S, Wang L, Stengel A, Rivier J, Taché Y. Brain somatostatin receptor 2 mediates the dipsogenic effect of central somatostatin and cortistatin in rats: role in drinking behavior. *Am J Physiol Regul Integr Comp Physiol*. 2014;307(7):R793–R801.
80. Gaykema RP, et al. Activation of murine pre-proglucagon-producing neurons reduces food intake and body weight. *J Clin Invest*.

- 2017;127(3):1031–1045.
81. Holt MK, et al. Preproglucagon neurons in the nucleus of the solitary tract are the main source of brain GLP-1, mediate stress-induced hypophagia, and limit unusually large intakes of food. *Diabetes*. 2019;68(1):21–33.
 82. Hisadome K, Reimann F, Gribble FM, Trapp S. Leptin directly depolarizes preproglucagon neurons in the nucleus tractus solitarius: electrical properties of glucagon-like peptide 1 neurons. *Diabetes*. 2010;59(8):1890–1898.
 83. Jelsing J, Vrang N, Raun K, Knudsen LB. Liraglutide induced anorexia is not mediated via brainstem GLP-1 neurons. *Diabetes*. 2011;60(suppl_1):297.
 84. Parker JA, et al. Glucagon and GLP-1 inhibit food intake and increase c-fos expression in similar appetite regulating centres in the brainstem and amygdala. *Int J Obes (Lond)*. 2013;37(10):1391–1398.
 85. St Andre J, Albanos K, Reilly S. C-fos expression in the rat brain following lithium chloride-induced illness. *Brain Res*. 2007;1135(1):122–128.
 86. Yamamoto T, Shimura T, Sako N, Azuma S, Bai WZ, Wakisaka S. C-fos expression in the rat brain after intraperitoneal injection of lithium chloride. *Neuroreport*. 1992;3(12):1049–1052.
 87. Essner RA, Smith AG, Jammik AA, Ryba AR, Trutner ZD, Carter ME. AgRP neurons can increase food intake during conditions of appetite suppression and inhibit anorexigenic parabrachial neurons. *J Neurosci*. 2017;37(36):8678–8687.
 88. Tokita K, Inoue T, Boughter JD. Afferent connections of the parabrachial nucleus in C57BL/6J mice. *Neuroscience*. 2009;161(2):475–488.
 89. Papas S, Ferguson AV. Electrophysiological characterization of reciprocal connections between the parabrachial nucleus and the area postrema in the rat. *Brain Res Bull*. 1990;24(4):577–582.
 90. Schaeffer M, et al. Rapid sensing of circulating ghrelin by hypothalamic appetite-modifying neurons. *Proc Natl Acad Sci U S A*. 2013;110(4):1512–1517.
 91. Campos CA, Bowen AJ, Han S, Wisse BE, Palmiter RD, Schwartz MW. Cancer-induced anorexia and malaise are mediated by CGRP neurons in the parabrachial nucleus. *Nat Neurosci*. 2017;20(7):934–942.
 92. Meek TH, et al. Functional identification of a neurocircuit regulating blood glucose. *Proc Natl Acad Sci U S A*. 2016;113(14):E2073–E2082.
 93. Wu Q, Clark MS, Palmiter RD. Deciphering a neuronal circuit that mediates appetite. *Nature*. 2012;483(7391):594–597.
 94. van der Kooy D, Koda LY. Organization of the projections of a circumventricular organ: the area postrema in the rat. *J Comp Neurol*. 1983;219(3):328–338.
 95. Betley JN, Cao ZF, Ritola KD, Sternson SM. Parallel, redundant circuit organization for homeostatic control of feeding behavior. *Cell*. 2013;155(6):1337–1350.
 96. Wu Q, Boyle MP, Palmiter RD. Loss of GABAergic signaling by AgRP neurons to the parabrachial nucleus leads to starvation. *Cell*. 2009;137(7):1225–1234.
 97. Wu Q, Palmiter RD. GABAergic signaling by AgRP neurons prevents anorexia via a melanocortin-independent mechanism. *Eur J Pharmacol*. 2011;660(1):21–27.
 98. Luquet S, Perez FA, Hnasko TS, Palmiter RD. NPY/AgRP neurons are essential for feeding in adult mice but can be ablated in neonates. *Science*. 2005;310(5748):683–685.
 99. Cone RD. Anatomy and regulation of the central melanocortin system. *Nat Neurosci*. 2005;8(5):571–578.
 100. Fan W, Ellacott KL, Halatchev IG, Takahashi K, Yu P, Cone RD. Cholecystokinin-mediated suppression of feeding involves the brainstem melanocortin system. *Nat Neurosci*. 2004;7(4):335–336.
 101. Piguet O, et al. Eating and hypothalamus changes in behavioral-variant frontotemporal dementia. *Ann Neurol*. 2011;69(2):312–319.
 102. Torres CV, et al. Long-term results of posteromedial hypothalamic deep brain stimulation for patients with resistant aggressiveness. *J Neurosurg*. 2013;119(2):277–287.